

Convolutional Normalizing Flows for Deep Gaussian Processes

Haibin Yu

Tencent

Shenzhen, China

haibin@u.nus.edu

Bryan Kian Hsiang Low

National University of Singapore

Republic of Singapore

lowkh@comp.nus.edu.sg

Patrick Jaillet

MIT

Cambridge, MA, USA

jaillet@mit.edu

Dapeng Liu

Tencent

Shenzhen China

rocliu@tencent.com

Abstract—Deep Gaussian processes (DGPs), a hierarchical composition of GP models, have successfully boosted the expressive power than the single-layer counterpart. However, it is impossible to perform exact inference in DGPs, which has motivated the recent development of variational inference based methods. Unfortunately, these methods either yield a biased posterior belief or are difficult to evaluate the convergence. This paper, on the contrary, introduces a new approach for specifying flexible, arbitrarily complex, and scalable approximate posterior distributions. The posterior distribution is constructed through a *normalizing flow* (NF) which transforms a simple initial probability into a more complex one through a sequence of invertible transformations. Moreover, a novel *convolutional normalizing flow* (CNF) is developed to improve the time efficiency and capture dependency between layers. Empirical evaluation demonstrates that CNF DGP outperforms the state-of-the-art approximation methods for DGPs.

Index Terms—Normalizing flow, Gaussian process, variational inference

I. INTRODUCTION

Gaussian processes (GPs) [1] have been widely applied in the machine learning community for the ability in providing closed-form predictions in the form of Gaussian distribution and formal measures of predictive uncertainty. Examples included but not limited to safety critical applications [2], computer vision [3], Bayesian optimization [4] and active learning [5]. However, the expressiveness of GP models are limited by the kernel functions which are challenging to design and often require expert knowledge for various complex tasks. To this end, recent years have witnessed the successfully composing GP models hierarchically into a multi-layer *deep* GP (DGP) model [6]–[12] which have boosted the expressive power significantly. Unfortunately, unlike the single-layer counterpart, DGPs do not entail tractable inference, which has motivated a series of approximate inference methods. Particularly, most previous works focus on *variational inference* (VI) [6], [7], [10], [13] by imposing Gaussian posterior assumptions. However, it has been pointed out by the work of [11] that the posterior belief demonstrates non-Gaussian patterns, hence potentially compromising the performance of the VI methods due to biased posterior estimation. To address this, the work of [11] proposed to utilize *Markov chain Monte Carlo* (MCMC) based sampling method to draw unbiased samples from the posterior belief. However, it is computational costly for generating samples in both training and prediction due to

its sequential sampling procedure, let alone the difficulty in evaluating the convergence.

To remedy the assumptions above, the work of [12] proposed the *implicit posterior variational inference* (IPVI) framework for DGP inference which can recover the unbiased posterior distribution efficiently. The method is inspired by the generative adversarial networks [14] which cast the DGP inference into a two-player game hoping to search for a Nash equilibrium. However, it is also mentioned in the paper that the Nash equilibrium is not guaranteed to retrieve.

This paper proposes a novel framework which utilizes the notion of *normalizing flows* [15]–[17] (NFs) which model the complex posterior distribution directly through a sequence of invertible neural networks. The benefits of choosing NFs are their expressiveness in modeling complex real-world data distributions which have been proven successful in supervised, semi-supervised, and unsupervised learning.

II. BACKGROUND AND RELATED WORK

Gaussian Process (GP). A GP defines a distribution over functions $f : \mathbb{R}^D \rightarrow \mathbb{R}$, for which any finite marginals follows a Gaussian distribution [1]. A GP is fully specified by its mean function which is often assumed to be zero and covariance (kernel) function $k : \mathbb{R}^D \times \mathbb{R}^D \rightarrow \mathbb{R}$. Given a set of N inputs $\mathbf{X} \triangleq \{\mathbf{x}_n\}_{n=1}^N$ and their corresponding noisy outputs $\mathbf{y} \triangleq \{y_n\}_{n=1}^N$ where $y_n \triangleq f(\mathbf{x}_n) + \varepsilon$ (corrupted by an i.i.d. Gaussian noise $\varepsilon \sim \mathcal{N}(0, \sigma_n^2)$). Then the set of latent outputs $\mathbf{f} \triangleq \{f(\mathbf{x}_n)\}_{n=1}^N$ follow a Gaussian distribution $p(\mathbf{f}) = \mathcal{N}(\mathbf{0}, \mathbf{K}_{\mathbf{XX}})$ where $\mathbf{K}_{\mathbf{XX}}$ denotes a covariance matrix with components $k(\mathbf{x}_n, \mathbf{x}'_n)$ for $n, n' = 1, \dots, N$. A widely used kernel function $k(\mathbf{x}_n, \mathbf{x}'_n)$ is the exponential quadratic or squared exponential (SE) with automatic relevance determination (ARD) $k_{\theta}(\mathbf{x}, \mathbf{x}') = \sigma_f^2 \exp(-0.5 \sum_{d=1}^D (x_d - x'_d)^2 / l_d^2)$ where l_d is the lengthscale for the d -th input dimension, σ_f^2 is the kernel variance and the kernel hyperparameters $\theta = (\{l_d\}_{d=1}^D, \sigma_f)$.

It follows that the marginal likelihood $p(\mathbf{y}) = \mathcal{N}(\mathbf{y} | \mathbf{0}, \mathbf{K}_{\mathbf{XX}} + \sigma_n^2 \mathbf{I})$. The GP posterior belief for the latent outputs $\mathbf{f}^* \triangleq \{f(\mathbf{x}^*)\}_{\mathbf{x}^* \in \mathbf{X}^*}$ can be computed analytically for any set \mathbf{X}^* test inputs following:

$$p(\mathbf{f}^* | \mathbf{y}) = \int p(\mathbf{f}^* | \mathbf{f}) p(\mathbf{f} | \mathbf{y}) d\mathbf{f}. \quad (1)$$

which can be written as

$$p(\mathbf{f}^*|\mathbf{y}) = \mathcal{N}(\boldsymbol{\mu}^*, \boldsymbol{\Sigma}^*)$$

where $\boldsymbol{\mu}^* = \mathbf{k}_{\mathbf{x}^* \mathbf{x}} (\mathbf{K}_{\mathbf{XX}} + \sigma_n^2 \mathbf{I})^{-1} \mathbf{y}$ and $\boldsymbol{\Sigma}^* = k_{\mathbf{x}^* \mathbf{x}^*} - \mathbf{k}_{\mathbf{x}^* \mathbf{x}} (\mathbf{K}_{\mathbf{XX}} + \sigma_n^2 \mathbf{I})^{-1} \mathbf{k}_{\mathbf{X} \mathbf{x}^*}$

Unfortunately, the inference procedure above incurs cubic time $\mathcal{O}(N^3)$, hence scaling poorly to massive datasets. To improve its scalability, the *sparse GP* (SGP) models spanned by the unifying view of [18] exploit a set $\mathbf{u} \triangleq \{u_m \triangleq f(\mathbf{z}_m)\}_{m=1}^M$ of inducing output variables for some small set $\mathbf{Z} \triangleq \{\mathbf{z}_m\}_{m=1}^M$ of inducing inputs (i.e., $M \ll N$). Then,

$$p(\mathbf{y}, \mathbf{f}, \mathbf{u}) = p(\mathbf{y}|\mathbf{f}) p(\mathbf{f}|\mathbf{u}) p(\mathbf{u}) \quad (2)$$

such that $p(\mathbf{f}|\mathbf{u}) = \mathcal{N}(\mathbf{f}|\mathbf{K}_{\mathbf{XZ}} \mathbf{K}_{\mathbf{ZZ}}^{-1} \mathbf{u}, \mathbf{K}_{\mathbf{XX}} - \mathbf{K}_{\mathbf{XZ}} \mathbf{K}_{\mathbf{ZZ}}^{-1} \mathbf{K}_{\mathbf{ZX}})$ where, with a slight abuse of notation, \mathbf{u} is treated as a column vector here, $\mathbf{K}_{\mathbf{XZ}} \triangleq \mathbf{K}_{\mathbf{ZX}}^\top$, and $\mathbf{K}_{\mathbf{ZZ}}$ and $\mathbf{K}_{\mathbf{ZX}}$ denote covariance matrices with components $k(\mathbf{z}_m, \mathbf{z}_{m'})$ for $m, m' = 1, \dots, M$ and $k(\mathbf{z}_m, \mathbf{x}_n)$ for $m = 1, \dots, M$ and $n = 1, \dots, N$, respectively. The SGP predictive belief can also be computed in closed form by marginalizing out \mathbf{u} : $p(\mathbf{f}^*|\mathbf{y}) = \int p(\mathbf{f}^*|\mathbf{u}) p(\mathbf{u}|\mathbf{y}) d\mathbf{u}$.

The work of [19] proposed a principled *variational inference* (VI) framework that approximates the joint posterior belief $p(\mathbf{f}, \mathbf{u}|\mathbf{y})$ with a variational posterior $q(\mathbf{f}, \mathbf{u}) \triangleq p(\mathbf{f}|\mathbf{u}) q(\mathbf{u})$ by minimizing the *Kullback-Leibler* (KL) divergence between them, which is equivalent to maximizing a lower bound of the log-marginal likelihood (i.e., also known as the *evidence lower bound* (ELBO)):

$$\text{ELBO} \triangleq \mathbb{E}_{q(\mathbf{f})} [\log p(\mathbf{y}|\mathbf{f})] - \text{KL}[q(\mathbf{u})||p(\mathbf{u})]$$

where $q(\mathbf{f}) \triangleq \int p(\mathbf{f}|\mathbf{u}) q(\mathbf{u}) d\mathbf{u}$.

Deep Gaussian Process (DGP). DGP composes multiple layers of GP models. Assume a DGP with a depth of L that each DGP layer is associated with a set $\mathbf{F}_{\ell-1}$ of inputs and a set \mathbf{F}_ℓ of outputs for $\ell = 1, \dots, L$ and $\mathbf{F}_0 \triangleq \mathbf{X}$. Let $\mathcal{F} \triangleq \{\mathbf{F}_\ell\}_{\ell=1}^L$, and the inducing inputs and corresponding inducing output variables for DGP layers $\ell = 1, \dots, L$ be denoted by the respective sets $\mathcal{Z} \triangleq \{\mathbf{Z}_\ell\}_{\ell=1}^L$ and $\mathcal{U} \triangleq \{\mathbf{U}_\ell\}_{\ell=1}^L$. Similar to the joint probability distribution of the SGP model in (2), the joint probability distribution of DGP can be written as:

$$p(\mathbf{y}, \mathcal{F}, \mathcal{U}) = \underbrace{p(\mathbf{y}|\mathbf{F}_L)}_{\text{data likelihood}} \underbrace{\left[\prod_{\ell=1}^L p(\mathbf{F}_\ell|\mathbf{U}_\ell) \right]}_{\text{DGP prior}} p(\mathcal{U}).$$

Similarly, the variational posterior is assumed to be $q(\mathcal{F}, \mathcal{U}) \triangleq \left[\prod_{\ell=1}^L p(\mathbf{F}_\ell|\mathbf{U}_\ell) \right] q(\mathcal{U})$, thus resulting in the following ELBO for the DGP model:

$$\text{ELBO} \triangleq \int q(\mathbf{F}_L) \log p(\mathbf{y}|\mathbf{F}_L) d\mathbf{F}_L - \text{KL}[q(\mathcal{U})||p(\mathcal{U})] \quad (3)$$

where

$$q(\mathbf{F}_L) \triangleq \int \prod_{\ell=1}^L p(\mathbf{F}_\ell|\mathbf{U}_\ell, \mathbf{F}_{\ell-1}) q(\mathcal{U}) d\mathbf{F}_1 \dots d\mathbf{F}_{L-1} d\mathcal{U}.$$

$q(\mathbf{F}_L)$ is computed with the use of reparameterization trick proposed in the work of [20] and Monte Carlo sampling method proposed in the work of [10].

Previous VI framework for DGP models [6], [7], [10], [13] have imposed the restrictive Gaussian mean-field assumption on $q(\mathcal{U})$. Unfortunately, it has been pointed by the work of [11] that the true posterior distribution of $q(\mathcal{U})$ usually exhibits a high correlation across the DGP layers and is non-Gaussian, hence potentially compromising the performance of such VI based DGP models. To further remove these assumptions, [12] proposed the IPVI framework for DGP that can capture the dependency between layers and ideally recover the unbiased posterior distribution. To achieve this, the method casts the DGP inference problem as a two-player game and search for a Nash equilibrium using *best response dynamics*¹ (BRD). However, the work of [21], [22] have pointed out the critical issue of convergence searching for Nash equilibrium. In fact, [12] also mentioned that there is no guarantee for BRD to converge to a Nash equilibrium, hence giving no assurance of recovering the true posterior distribution.

The optimal goal for DGP inference lies in three aspect: recovery of the true posterior, convergence analysis, and time efficiency. To achieve this, this paper proposes a novel framework based on the idea of *convolutional normalizing flows* (CNF) to model the posterior distribution directly and efficiently, as detailed in Section III.

III. CONVOLUTIONAL NORMALIZING FLOW FOR DGPs

Normalizing Flows By examining the ELBO in Eq. 3 in detail, we can find out that maximum of the ELBO is achieved when $\text{KL}[q(\mathcal{U})||p(\mathcal{U}|\mathbf{y})] = 0$. Our optimal goal is to develop an ideal family of variational distributions $q(\mathcal{U})$ that is highly flexible enough to represent the true posterior distribution. Here the notion of *normalizing flow* [15], [16] (NF) comes in. An NF describes the transformation of a simple distribution into a complex distribution by repeated applying a sequence of invertible mappings. Following the *change of variable* rule, the NF framework can be described as: given a random variable $\mathbf{z} \in \mathbb{R}^D$ with distribution $\pi(\mathbf{z})$. There exists an invertible and smooth mapping $f : \mathbb{R}^D \rightarrow \mathbb{R}^D$, then the resulting random variable $\mathbf{x} = f(\mathbf{z})$ has a distribution:

$$p(\mathbf{x}) = \pi(\mathbf{z}) \left| \det \left(\frac{d\mathbf{z}}{d\mathbf{x}} \right) \right| = \pi(\mathbf{z}) \left| \det [f'(\mathbf{z})] \right|^{-1}$$

where $\left| \det [f'(\mathbf{z})] \right|^{-1}$ is the absolute value of the determinant of the Jacobian of f evaluated at \mathbf{z} .

Remark 1: It has been proved that certain NFs are universal approximators [23], [24]. In other words, it means with careful design of the mapping f , we can transform a simple distribution into any complex distribution².

Recall that maximizing the ELBO is equivalent to minimizing the KL divergence. Specifically, the KL divergence between our variational posterior $q(\mathcal{U})$ and the true posterior

¹This procedure is sometimes called “better-response dynamics” (<http://timroughgarden.org/f13/l116.pdf>).

²We refer the readers to [23]–[27] for a detailed discussion of the proof.

$p(\mathcal{U}|\mathbf{y})$. Following the *Bayes' theorem*, the posterior distribution can be written as:

$$p(\mathcal{U}|\mathbf{y}) = \frac{p(\mathbf{y}|\mathbf{F}_L, \mathcal{U})p(\mathcal{U})}{p(\mathbf{y}|\mathbf{F}_L)}. \quad (4)$$

Similarly, \mathbf{F}_L is a Monte Carlo sample from the predictive distribution of the layer outputs: $\mathbf{F}_L \sim \int \prod_{\ell=1}^{L-1} p(\mathbf{F}_\ell|\mathbf{U}_\ell, \mathbf{F}_{\ell-1})d\mathbf{F}_\ell$. Inspired by the idea of NF, we propose to construct the variational posterior $q(\mathcal{U})$ through a sequence of invertible and smooth mappings: $\mathcal{G} : \mathcal{V} \rightarrow \mathcal{U}$. Here \mathcal{V} is a new random variable with distribution $\pi(\cdot)$, then according to the *change of variable* rule:

$$q(\mathcal{U}) = \pi(\mathcal{V}) \times \left| \det \left(\frac{d\mathcal{G}}{d\mathcal{V}} \right) \right|^{-1}. \quad (5)$$

Using (5), the KL divergence can be re-written as:

$$\begin{aligned} \text{KL}(q(\mathcal{U})||p(\mathcal{U}|\mathbf{y})) &= \text{KL} \left(q(\mathcal{U}) \parallel \frac{p(\mathbf{y}|\mathbf{F}_L, \mathcal{U})p(\mathcal{U})}{p(\mathbf{y}|\mathbf{F}_L)} \right) \\ &= \int q(\mathcal{U}) \left[\log \frac{q(\mathcal{U})}{p(\mathbf{y}|\mathbf{F}_L, \mathcal{U})p(\mathcal{U})} \right] d\mathcal{U} + \log p(\mathbf{y}|\mathbf{F}_L) \\ &= \mathbb{E}_{q(\mathcal{U})} [\log q(\mathcal{U}) - \log p(\mathbf{y}|\mathbf{F}_L, \mathcal{U}) - p(\mathcal{U})] + \log p(\mathbf{y}|\mathbf{F}_L) \\ &= \mathbb{E}_{\pi(\mathcal{V})} \left[\log \pi(\mathcal{V}) - \log \left| \det \left(\frac{d\mathcal{G}}{d\mathcal{V}} \right) \right| - \log p(\mathbf{y}|\mathbf{F}_L, \mathcal{G}(\mathcal{V})) \right. \\ &\quad \left. - \log p(\mathcal{G}(\mathcal{V})) \right] + \text{const} \end{aligned} \quad (6)$$

Remark 2: Note that the IPVI DGP framework in [12] represents the variational posterior implicitly with samples. Hence, to compute the log-density ratio in the KL divergence, it resorts to a *discriminator* to output a function value to represent it. However, in our NF framework, the log-density for the variational posterior $\log q(\mathcal{U}) = \log \pi(\mathcal{V}) - \log |\det(d\mathcal{G}/d\mathcal{V})|$ results in an analytical solution.

Convolutional Normalizing Flows Here we discuss how the architecture of the normalizing flow is designed for DGP. A naive design is to consider a layer-wise normalizing flow which is illustrated in Figure 1. However, such a naive design suffers from the following critical issues:

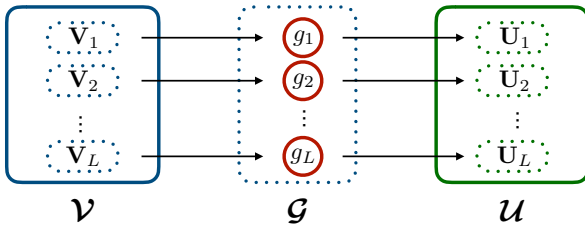


Fig. 1. A naive design of normalizing flow for DGP. The normalizing flow \mathcal{G} is separated into L individual flows.

- Figure 1 shows that to recover the posterior samples of M different inducing variables $\mathbf{u}_{\ell 1}, \dots, \mathbf{u}_{\ell M}$ ($\mathbf{U}_\ell = \{\mathbf{u}_{\ell 1}, \dots, \mathbf{u}_{\ell M}\}$) where $\mathbf{u}_{\ell 1} \in \mathbb{R}^{d_\ell}$, it is natural to design the normalizing flow $g_\ell : \mathbb{R}^{M d_\ell} \rightarrow \mathbb{R}^{M d_\ell}$. Therefore, a large

number of parameters is needed, which will increase the risk of overfitting.

- Another critical issue is the computational complexity. In general, computing the log Jacobian determinant incurs $\mathcal{O}(M^3 \cdot d_\ell^3)$, hence resulting in the difficulty in optimization.

- Such a design fails to capture the dependency of the inducing output variables \mathbf{U}_ℓ among different layers. As pointed out by [12], the posterior distribution of $p(\mathcal{U}|\mathbf{y})$ is highly correlated among layers.

- Such a design fails to adequately capture the dependency of the inducing output variables \mathbf{U}_ℓ on its corresponding inducing inputs \mathbf{Z}_ℓ , hence restricting its capability to model the output posterior \mathcal{U} accurately.

To resolve the above issues, we propose a novel normalizing flow architecture with convolution for DGP models, as shown in Figure 2. Instead of treating $\mathcal{V} = \{\mathbf{V}_1, \mathbf{V}_2, \dots, \mathbf{V}_L\}$ separately, we decide to stack $\{\mathbf{V}_1, \mathbf{V}_2, \dots, \mathbf{V}_L\}$ to be a three-dimensional tensor denoted as:

$$\mathcal{V} \in \mathbb{R}^{M \times 1 \times \sum_{\ell=1}^L d_\ell} \quad (7)$$

and design our normalizing flow $\mathcal{G} : \mathbb{R}^{M \times 1 \times \sum_{\ell=1}^L d_\ell} \rightarrow \mathbb{R}^{M \times 1 \times \sum_{\ell=1}^L d_\ell}$ accordingly as shown in Figure 2.

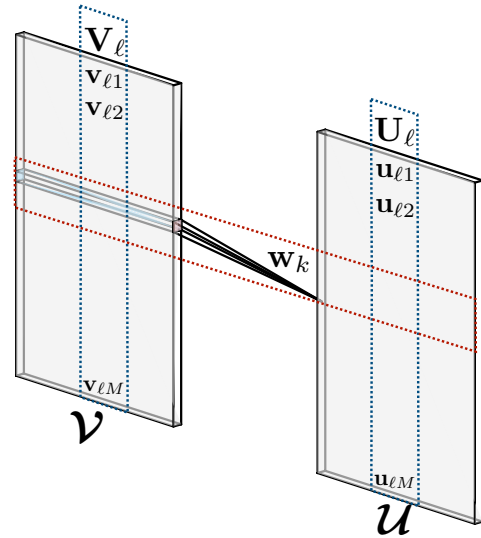


Fig. 2. The normalizing flow with convolution for DGP. The kernel tensor \mathbf{W} can be decomposed into a set of tensors $\{\mathbf{w}_1, \mathbf{w}_2, \dots, \mathbf{w}_K\}$ where $\mathbf{w}_1 \in \mathbb{R}^{1 \times 1 \times \sum_{\ell=1}^L d_\ell}$ $K = \sum_{\ell=1}^L d_\ell$. The red box indicates the convolution with \mathbf{w}_k .

To this end, we propose to convolve \mathcal{V} with a kernel tensor \mathbf{W} where $\mathbf{W} \in \mathbb{R}^{1 \times 1 \times \sum_{\ell=1}^L d_\ell \times \sum_{\ell=1}^L d_\ell}$ as shown in Figure 2. In this way, the normalizing flow \mathcal{G} is fully characterized by the kernel tensor \mathbf{W} with a significantly smaller number of parameters. Hence the log Jacobian determinant can be easily written as:

$$\log \left| \det \left(\frac{d\mathcal{G}}{d\mathcal{V}} \right) \right| = M \times 1 \times \log |\det(\mathbf{W})| \quad (8)$$

Remark 3: Note that compared with the naive design in Figure 1, computing the log Jacobian determinant only incurs

$\mathcal{O}\left(\left(\sum_{\ell=1}^L d_{\ell}\right)^3\right)$, which reduces the time complexity by $\mathcal{O}(M^3)$ times. Moreover, compared with the naive design, it is also easier to compute the determinant of \mathbf{W} . Another advantage is that the kernel tensor \mathbf{W} naturally captures the dependency of inducing variables $\{\mathbf{U}_1, \mathbf{U}_2, \dots, \mathbf{U}_L\}$ between layers.

Furthermore, to capture the dependency of the inducing output variables \mathbf{U}_{ℓ} on its corresponding inducing inputs \mathbf{Z}_{ℓ} , we manually construct the base distribution $\pi(\mathbf{V})$ to depend on the inducing inputs \mathcal{Z} . For each layer ℓ , the base distribution can be written:

$$\mathbf{V}_{\ell} \sim \mathcal{N}(\boldsymbol{\mu}_{\ell}, \boldsymbol{\sigma}_{\ell}), \text{ where } [\boldsymbol{\mu}_{\ell}, \boldsymbol{\sigma}_{\ell}] = \varphi_{\ell}(\mathbf{Z}_{\ell}) \quad (9)$$

where φ_{ℓ} is a neural network. We represent φ_{ℓ} using a two-layer neural network with hidden dimension being 256 and leaky ReLU activation in the middle. Note that it utilizes separate set of parameters for different layer ℓ . We observe from our experiments that our normalizing flow for DGP with convolutions improves the performance considerably, which will be shown in Section IV.

IV. EXPERIMENTS AND DISCUSSIONS

A. Regression

UCI Benchmark Regression. Our experiments are first conducted on 7 UCI benchmark regression datasets. We have performed a random 0.9/0.1 train/test split.

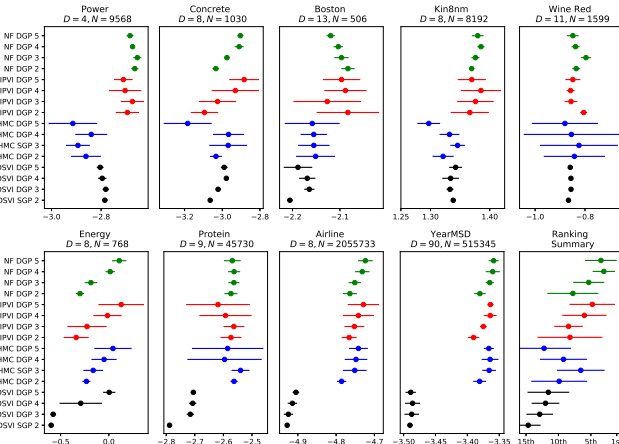


Fig. 3. Mean test log-likelihood and standard deviation achieved by our NF framework (green), IPVI (red), SGHMC (blue), and DSVI (black) for DGPs for UCI benchmark and large-scale regression datasets. Higher test log-likelihood (i.e., to the right) is better.

Large-Scale Regression. We then evaluate the performance of NF on two real-world large-scale regression datasets: (a) YearMSD dataset with a large input dimension $D = 90$ and data size $N \approx 500000$, and (b) Airline dataset with input dimension $D = 8$ and a large data size $N \approx 2$ million. For YearMSD dataset, we use the first 463715 examples as training data and the last 51630 examples as test data. For Airline dataset, we set the last 100000 examples as test data.

In the above regression tasks, the performance metric is the *mean test log-likelihood* (MLL). Figure 3 shows the results of the mean test log-likelihood and standard deviation over

10 runs. It can be observed that NF generally outperforms other frameworks and the ranking summary shows that our NF framework for a 4-layer DGP model (NF DGP 4) performs the best on average across all regression tasks. For large-scale regression tasks, the performance of NF consistently increases with a greater depth.

Evaluation of ELBO. To further demonstrate the expressiveness of the NF framework, we have also computed the estimate of training ELBO for NF DGP and IPVI DGP models on Boston dataset. Table I shows the mean ELBOs of NF and IPVI over 10 runs for the Boston dataset. NF generally achieves higher ELBOs, which agrees with results of the test MLL in Fig. 3.

TABLE I
MEAN ELBOs FOR BOSTON DATASET.

Model	NF	IPVI
DGP 2	-836.48	-846.65
DGP 3	-814.13	-846.45
DGP 4	-762.54	-776.93
DGP 5	-734.23	-758.42

Remark 4: As it can be observed from Figure 3, the results of NF DGP are very robust across different runs (as can be seen from the smaller standard deviations) compared with SGHMC and IPVI which represent the posterior distribution with samples. Moreover, Table I clearly demonstrates that NF works better in recovering the true posterior distribution than IPVI. The inferior performance for IPVI is due to the convergence issue mentioned previously.

Time efficiency. Table II shows the time efficiency of NF DGP with respect to IPVI DGP and NF DGP.

TABLE II
INCURRED TIME BY A 5-LAYER DGP MODEL FOR AIRLINE DATASET

	NF DGP	IPVI DGP	SGHMC DGP
Average training time	0.56 sec	0.42 sec	3.67 sec
Average generation time	0.32 sec	0.31 sec	156.2 sec

Remark 5: As we can observe from Table II, the average training time and generation time for NF DGP is slightly longer than IPVI DGP. Compared with respect to the predictive performance in Fig 3, it is an acceptable trade-off since NF has no issue in terms of convergence.

B. Classification

We evaluate the performance of NF in three classification tasks using the real-world MNIST, fashion-MNIST, and CIFAR-10 datasets. Both MNIST and fashion-MNIST datasets are grey-scale images of 28×28 pixels. The CIFAR-10 dataset consists of colored images of 32×32 pixels. We utilize a 4-layer DGP model with 100 inducing inputs per layer and a robust-max multiclass likelihood [28].

Convolutional Skip-layer Connection (CSC): For the image datasets, the data distribution has local correlation between pixels. It would be better if the skip-layer connection can incorporate such information as a base for invariant mapping.

We change the skip-layer connection from a fully connected manner to a convolutional manner, \mathbf{W} is convolution kernel with height and width of 3×3 . Note that in CSC, \mathbf{W} is trainable.. Results show that the CSC boosts the DGP performance in real world image datasets and performs best when integrated with NF.

We also change the skip-layer connection to be CSC. Table III shows that the CSC boosts the DGP performance in real world image datasets and performs best when integrated with the NF framework.

TABLE III

MEAN TEST ACCURACY (%) ACHIEVED BY NF, IPVI, SGHMC, AND DSVI FOR 3 CLASSIFICATION DATASETS WITH CONVOLUTIONS.

Dataset	MNIST		Fashion-MNIST		CIFAR-10	
	SGP	DGP 4	SGP	DGP 4	SGP	DGP 4
DSVI	97.32	99.16	86.98	91.57	47.15	75.05
SGHMC	96.41	98.15	85.84	88.14	47.32	70.78
IPVI	97.02	99.32	87.29	91.78	48.07	76.11
NF	97.37	99.43	87.14	92.03	48.13	76.81

V. CONCLUSION

This paper proposes a novel NF framework for DGPs inference which is targeted to resolve the biased mean-field Gaussian approximation and critical issue of convergence in IPVI. We also propose a novel convolutional NF (CNF) architecture for DGPs to better capture dependency between inducing variables and speed up training. Empirical evaluation shows that CNF performs better than other state-of-the-art approximation methods for DGPs in regression and classification tasks. For future work, we plan to extend the CNF framework for DGP to the area of semi-supervised learning to incorporate the generative expressiveness of *normalizing flows*.

REFERENCES

- [1] C. E. Rasmussen and C. K. Williams, *Gaussian processes for machine learning*. MIT Press, 2006.
- [2] D. Reeb, A. Doerr, S. Gerwinn, and B. Rakitsch, “Learning Gaussian processes by minimizing Pac-Bayesian generalization bounds,” in *Proc. NeurIPS*, 2018, pp. 3337–3347.
- [3] M. van der Wilk, C. E. Rasmussen, and J. Hensman, “Convolutional Gaussian processes,” in *Proc. NeurIPS*, 2017, pp. 2849–2858.
- [4] N. Srinivas, A. Krause, S. M. Kakade, and M. Seeger, “Gaussian process optimization in the bandit setting: No regret and experimental design,” *Proc. ICML*, pp. 1015–1022, 2010.
- [5] C. Zimmer, M. Meister, and D. Nguyen-Tuong, “Safe active learning for time-series modeling with Gaussian processes,” in *Proc. NeurIPS*, 2018, pp. 2730–2739.
- [6] A. Damianou and N. Lawrence, “Deep Gaussian processes,” in *Proc. AISTATS*, 2013, pp. 207–215.
- [7] J. Hensman and N. D. Lawrence, “Nested variational compression in deep Gaussian processes,” arXiv:1412.1370, 2014.
- [8] T. Bui, D. Hernández-Lobato, J. Hernandez-Lobato, Y. Li, and R. Turner, “Deep Gaussian processes for regression using approximate expectation propagation,” in *Proc. ICML*, 2016, pp. 1472–1481.
- [9] K. Cutajar, E. V. Bonilla, P. Michiardi, and M. Filippone, “Random feature expansions for deep Gaussian processes,” in *Proc. ICML*, 2017, pp. 884–893.
- [10] H. Salimbeni and M. Deisenroth, “Doubly stochastic variational inference for deep Gaussian processes,” in *Proc. NeurIPS*, 2017, pp. 4588–4599.
- [11] M. Havasi, J. M. Hernández-Lobato, and J. J. Murillo-Fuentes, “Inference in deep Gaussian processes using stochastic gradient Hamiltonian Monte Carlo,” in *Proc. NeurIPS*, 2018, pp. 7517–7527.
- [12] H. Yu, Y. Chen, Z. Dai, K. H. Low, and P. Jaillet, “Implicit posterior variational inference for deep Gaussian processes,” in *Proc. NeurIPS*, 2019, pp. 14475–14486.
- [13] Z. Dai, A. Damianou, J. González, and N. Lawrence, “Variational auto-encoded deep Gaussian processes,” in *Proc. ICLR*, 2016.
- [14] I. Goodfellow, J. Pouget-Abadie, M. Mirza, B. Xu, D. Warde-Farley, S. Ozair, A. Courville, and Y. Bengio, “Generative adversarial nets,” in *Proc. NeurIPS*, 2014, pp. 2672–2680.
- [15] E. G. Tabak and E. Vanden-Eijnden, “Density estimation by dual ascent of the log-likelihood,” *Communications in Mathematical Sciences*, vol. 8, no. 1, pp. 217–233, 2010.
- [16] E. G. Tabak and C. V. Turner, “A family of nonparametric density estimation algorithms,” *Communications on Pure and Applied Mathematics*, vol. 66, no. 2, pp. 145–164, 2013.
- [17] D. Rezende and S. Mohamed, “Variational inference with normalizing flows,” in *Proc. ICML*, 2015, pp. 1530–1538.
- [18] J. Quiñonero-Candela and C. E. Rasmussen, “A unifying view of sparse approximate Gaussian process regression,” *The Journal of Machine Learning Research*, vol. 6, pp. 1939–1959, 2005.
- [19] M. Titsias, “Variational learning of inducing variables in sparse Gaussian processes,” in *Proc. AISTATS*, 2009, pp. 567–574.
- [20] D. P. Kingma and M. Welling, “Auto-encoding variational Bayes,” in *Proc. ICLR*, 2013.
- [21] I. Goodfellow, “NIPS 2016 tutorial: Generative adversarial networks,” arXiv:1701.00160, 2016.
- [22] T. Salimans, I. Goodfellow, W. Zaremba, V. Cheung, A. Radford, and X. Chen, “Improved techniques for training gans,” in *Proc. NeurIPS*, 2016, pp. 2234–2242.
- [23] C.-W. Huang, D. Krueger, A. Lacoste, and A. Courville, “Neural autoregressive flows,” in *Proc. ICML*, 2018, pp. 2078–2087.
- [24] P. Jaini, I. Kobyzev, M. Brubaker, and Y. Yu, “Tails of triangular flows,” arXiv:1907.04481, 2019.
- [25] C. Villani, *Topics in optimal transportation*. American Mathematical Society, 2003, no. 58.
- [26] V. I. Bogachev, A. V. Kolesnikov, and K. V. Medvedev, “Triangular transformations of measures,” *Matematicheskii Sbornik*, vol. 196, no. 3, pp. 3–30, 2005.
- [27] K. V. Medvedev, “Certain properties of triangular transformations of measures,” *Theory of Stochastic Processes*, vol. 14, no. 1, pp. 95–99, 2008.
- [28] D. Hernández-Lobato, J. M. Hernández-Lobato, and P. Dupont, “Robust multi-class Gaussian process classification,” in *Proc. NeurIPS*, 2011, pp. 280–288.